

DUFFING-TYPE EQUATIONS: SINGULAR POINTS OF AMPLITUDE PROFILES AND BIFURCATIONS

JAN KYZIOŁ, ANDRZEJ OKNIŃSKI

Politechnika Świętokrzyska
Al. 1000-lecia Państwa Polskiego 7, 25-314 Kielce, Poland

(Received May 1, 2021; accepted August 30, 2021)

We study the Duffing equation and its generalizations with polynomial non-linearities. Recently, we have demonstrated that metamorphoses of the amplitude-response curves, computed by asymptotic methods in implicit form as $F(\Omega, A) = 0$, permit prediction of qualitative changes of dynamics occurring at singular points of the implicit curve $F(\Omega, A) = 0$. In the present work, we determine a global structure of singular points of the amplitude profiles computing bifurcation sets, *i.e.* sets containing all points in the parameter space for which the amplitude profile has a singular point. We connect our work with independent research on tangential points on amplitude profiles, associated with jump phenomena, characteristic for the Duffing equation. We also show that our techniques can be applied to solutions of the form of $\Omega_{\pm} = f_{\pm}(A)$, obtained within other asymptotic approaches.

DOI:10.5506/APhysPolB.52.1239

1. Introduction and motivation

Recently, non-linear Duffing-type oscillators attracted considerable attention due to a rich variety of applications. A very interesting class of Mathieu–van der Pol–Duffing oscillators with polynomial non-linearities is described by the following equation:

$$m \frac{d^2x}{dt^2} + (\mu + \lambda x^2) \frac{dx}{dt} + (k_1 + b \cos(\bar{\omega}t + \phi)) x + \sum_{j=2}^n k_j x^j = a \cos(\omega t), \quad (1)$$

which, for example, can model dynamics of a mathematical pendulum or a ship-roll motions [1–10]. In the case of mechanical vibrations ($\lambda = b = 0$),

m is the mass, μ is the damping parameter, k_1 can be interpreted as the linear stiffness coefficient, k_n ($n = 2, 3, 4, \dots$) are parameters of the non-linear restoring force, while a , ω are the amplitude and angular frequency of the periodic driving force, respectively.

Applications of the Duffing-type equations are not limited to purely mechanical systems. More precisely, Eq. (1) is used to model dynamics of micro/nano electromechanical systems [11, 12], plasma oscillations [13–15], high-intensity discharge lamps [16], optical solitons in plasma [17], quasi-periodic dynamics of Bose–Einstein condensates in periodic lattices [18, 19], non-linear dynamics of polarization oscillations [20], and ion dynamics in the Paul traps [21].

Let us consider, for the sake of a motivating example, non-linear dynamics of plasma oscillations [14]. The model consists of a set of fluid equations for the electrons and ions plus the complete set of Maxwell’s equations. The authors show that dynamics is effectively governed by Eq. (1) with non-zero parameters $\underline{c} = (m, \mu, \lambda, k_1, k_2, k_3, a, \omega)$. The authors compute an approximate non-linear resonance of the form of $A \cos(\omega t + \varphi) + \text{const.}$ and the corresponding highly non-linear implicit amplitude–frequency response equation of the form of $F(\omega, A, \underline{c}) = 0$ (cf. Eq. (25) in [14]). It turns out that bifurcations of plasma dynamics, such as hysteresis and jump phenomenon, related to appearance/disappearance of branches of solutions, are determined by the $F(\omega, A, \underline{c}) = 0$ equation [13, 14]. The aim of the present work is to show how information about such bifurcations, as well as more complicated ones, can be extracted analytically from amplitude–frequency equations (see Appendix C for application of our approach to the amplitude–frequency response equation obtained in [13]).

Nonlinear responses of the form of $x(t) = A(\omega) \cos(\omega t + \varphi(\omega))$ can be computed by any of many asymptotic methods [22]. In the present work, we compute the asymptotic solutions in an implicit form as $F(\omega, A, \underline{c}) = 0$, where $\underline{c} = (c_1, c_2, \dots, c_m)$ are parameters, by the application of the Krylov–Bogoliubov–Mitropolsky (KBM) method [22].

As explained in Section 3 and demonstrated in our earlier papers, qualitative changes of dynamics occur at singular points of the implicit amplitude equation $F(\omega, A, \underline{c}) = 0$ (also known as the amplitude–frequency response or the amplitude-response equation), see [23] and references therein. Singular points appear at some special values of parameters $\underline{c} = \underline{c}_*$, for which the implicit function F fulfills appropriate equations, see Eqs. (13). In other words, at $\underline{c} = \underline{c}_*$, there is a change of differential properties of the amplitude-response curve $F(\omega, A, \underline{c}_*) = 0$ at a singular point (ω_*, A_*) , referred to as a metamorphosis.

In this work, we attempt to find a global picture of singular points of the amplitude-response equation for the generalized Duffing equation (1). We derive formulae for singular points and the bifurcation set in the general case and apply these results to the case of the standard cubic Duffing equation ($n = 3$) and to the cubic-quintic Duffing equation ($n = 5$). We shall carry out this program for higher values of n in our future work.

In Section 7, we connect our work on singular metamorphoses with research on changes of differential properties of amplitude–frequency response curves in a non-singular case, which can be viewed as non-singular metamorphoses [2]. Metamorphoses described in [2] can be classified as vertical tangencies — for some parameter values, the amplitude-response curve has vertical tangent points (critical but non-singular) associated with saddle-node bifurcations (jump phenomena) [2].

In Appendix A, we analyse metamorphoses of the amplitude profiles from another point of view. Implicit equation $F(\Omega, A) = 0$ can be solved for Ω for the generalized Duffing equation so that we can get explicit solutions $\Omega_{\pm} = f_{\pm}(A)$. Intersection conditions for these two branches, $f_+(A) = f_-(A)$, yield singular points of the amplitude profile (the same as described in Section 4.3, obtained within the more general approach of Section 4.2). We present a more detailed picture of transformation of a non-singular amplitude profile into a self-intersection, non-singular amplitude, and into amplitude with an isolated point.

We also apply our approach to explicit solutions $\omega_{\pm} = g_{\pm}(A)$ computed in [5] for the cubic-quintic oscillator obtained via the Multiple Scales Linstedt Poincaré (MSLP) method, see Appendix B. We show that our techniques, described in Section 4 as well as in Appendix A, can be applied to amplitudes obtained within another asymptotic approach. Application of our approach to plasma equations is described in Appendix C.

Finally, in Appendix D, computational details are described.

2. The Krylov–Bogoliubov–Mitropolsky amplitude profiles for the generalized Duffing equation

In this work, we put in Eq. (1) $\lambda = b = 0$ and consider only odd values of j . Introducing non-dimensional units, $\Omega = \frac{\omega}{\omega_n}$, $\omega_n = \sqrt{\frac{k_1}{m}}$, $\tau = \omega_n t$, Eq. (1) is cast into the form of

$$\ddot{y} + h\dot{y} + y + c_3y^3 + c_5y^5 + \dots + c_ny^n = f \cos(\Omega\tau), \tag{2}$$

where overdots denote derivatives with respect to τ , $n = 3, 5, 7, 9, \dots$. We assume that parameters h, c_3, \dots, c_n, f are small and can be thus written as $h = \varepsilon\bar{h}$, $c_3 = \varepsilon\bar{c}_3$, \dots , $c_n = \varepsilon\bar{c}_n$, $f = \varepsilon\bar{f}$, where ε is a small parameter and $\bar{h}, \bar{c}_3, \dots, \bar{c}_n, \bar{f}$ are of the order of $O(1)$.

Looking for 1 : 1 resonances, we rewrite Eq. (2) in the form of a weakly perturbed system

$$\frac{d^2y}{d\tau^2} + \Omega^2 y + \varepsilon (\sigma y + g) = 0, \tag{3}$$

where

$$g = \bar{h} \frac{dy}{d\tau} + \bar{c}_3 y^3 + \bar{c}_5 y^5 + \dots + \bar{c}_n y^n - \bar{f} \cos(\Omega\tau), \tag{4a}$$

$$\varepsilon\sigma = 1 - \Omega^2, \tag{4b}$$

and $\sigma = O(1)$.

We apply the Krylov–Bogoliubov–Mitropolsky (KBM) perturbation approach [22] assuming the 1 : 1 resonance in the form of

$$y = A(\tau) \cos(\Omega\tau + \varphi(\tau)) + \varepsilon y_1(A, \varphi, \tau) + \dots \tag{5}$$

with slowly varying amplitude A and phase φ

$$\frac{dA}{d\tau} = \varepsilon M_1(A, \varphi) + \dots, \tag{6a}$$

$$\frac{d\varphi}{d\tau} = \varepsilon N_1(A, \varphi) + \dots, \tag{6b}$$

obtaining

$$M_1 = \frac{1}{2\Omega} (-\bar{h}A\Omega - \bar{f} \sin \varphi), \tag{7a}$$

$$N_1 = \frac{1}{2\Omega A} (\sigma A + \bar{d}_3 A^3 + \bar{d}_5 A^5 + \dots \bar{d}_n - \bar{f} \cos \varphi), \tag{7b}$$

with \bar{d}_n given in (9).

The fixed points of the slow-flow equations (6), (7) correspond to solutions with constant amplitude and phase [2]. We thus demand that $M_1 = N_1 = 0$, eliminate φ , and get the following implicit amplitude–frequency equation:

$$\begin{aligned} L(X, Y) &= h^2 XY + Y (X - 1 - d_3 Y - d_5 Y^2 - \dots - d_n Y^n)^2 - f^2 = 0, \\ X &\equiv \Omega^2, \quad Y \equiv A^2 \end{aligned} \tag{8}$$

and

$$\bar{d}_n = 2^{\frac{1-n}{2}} \frac{n!!}{\left(\frac{n+1}{2}\right)!} \bar{c}_n, \quad n = 3, 5, 7, 9, \dots \tag{9}$$

In what follows, we shall also write $F(\Omega, A) = L(\Omega^2, A^2)$.

3. Singular points of amplitude profiles and bifurcations of dynamics

Singular points of amplitude profiles were first described in [24]. A detailed description of properties and applications of singular points of amplitude profiles can be found in [23]. In short, solving a non-linear differential equation of the form of

$$\frac{d^2y}{d\tau^2} + \omega^2 y = \varepsilon f\left(y, \frac{dy}{d\tau}, \tau\right), \tag{10}$$

where ε is a small parameter and f is a periodic function of time τ with period $T = \frac{2\pi}{\Omega}$ by an asymptotic method, we find an approximate solution

$$y(\tau) = A(\Omega) \cos(\Omega\tau + \varphi(\Omega)) + \varepsilon y_1(\tau) + \dots, \tag{11}$$

where the amplitude A and frequency Ω fulfill the amplitude-response equation

$$F(\Omega, A; \underline{c}) = 0, \tag{12}$$

where $\underline{c} = (c_1, c_2, \dots, c_m)$ are parameters. Equation (12) defines an implicit function — a two-dimensional planar curve — the amplitude–frequency response curve (the amplitude profile). The form of this curve, as well as the stability of solution (11), determine (approximately) dynamics of the system.

Qualitative changes of shape of the amplitude profile (12), which are equivalent to changes of differential properties of these curves and are referred henceforth as metamorphoses, induced by smooth changes of control parameters \underline{c} , lead to qualitative changes of dynamics (bifurcations). According to the differential geometry of curves [25, 26], an implicit curve changes its form at singular points which fulfill the following equations:

$$F(\Omega, A; \underline{c}) = 0, \tag{13a}$$

$$\frac{\partial F(\Omega, A; \underline{c})}{\partial \Omega} = 0, \tag{13b}$$

$$\frac{\partial F(\Omega, A; \underline{c})}{\partial A} = 0. \tag{13c}$$

Solutions of Eqs. (13), if exist, are of the form of $\Omega = \Omega_*, A = A_*, \underline{c} = \underline{c}_*$. Accordingly, the amplitude-response curve $F(\Omega, A, \underline{c}_*) = 0$ changes its differential properties at singular point (Ω_*, A_*) .

Metamorphoses of the amplitude–frequency curves (*i.e.* changes of differential properties) can also occur in a non-singular setting. More precisely, a metamorphosis of this kind occurs when a smooth change of parameters \underline{c}

leads to the formation of vertical tangent points of an amplitude profile. This gives rise to the so-called jump phenomenon, first described in the context of the change of differential properties of the amplitude-response curve for the cubic Duffing equation in [2]. It follows that equations guaranteeing the formation of a (non-singular) vertical tangent point (Ω_*, A_*) are

$$F(\Omega, A; \underline{c}) = 0, \quad (14a)$$

$$\frac{\partial F(\Omega, A; \underline{c})}{\partial A} = 0, \quad (14b)$$

see Section 7 for more details.

Investigation of metamorphoses of amplitude profiles induced by the change of parameters was carried out in the framework of Catastrophe Theory in [27] for the Duffing equation in a non-singular case. The idea to use Implicit Function Theorem to “define and find different branches intersecting at singular points” of amplitude profiles was proposed in [28].

While changes of differential properties of asymptotic solutions are important, stability of the solutions is another essential factor shaping the dynamics. Stability of the slow-flow equations (6) is determined by eigenvalues of the Jacobian matrix [29]

$$\mathbb{J} = \begin{pmatrix} \frac{\partial M_1}{\partial A} & \frac{\partial M_1}{\partial \varphi} \\ \frac{\partial N_1}{\partial A} & \frac{\partial N_1}{\partial \varphi} \end{pmatrix}. \quad (15)$$

We show in Section 7 that changes of differential properties of asymptotic solutions and changes of their stability (bifurcations) are strictly related.

4. Global view of metamorphoses of the amplitude profiles: general case and examples for $n = 3, 5$

4.1. Singular points

We shall investigate singular points of the amplitude equation (8) because bifurcations occur at these points, cf. Section 3. Singular points of algebraic curve $L_n(X, Y) = 0$ are given by equations

$$L_n(X, Y) = 0, \quad (16a)$$

$$\frac{\partial L_n(X, Y)}{\partial X} = 0, \quad (16b)$$

$$\frac{\partial L_n(X, Y)}{\partial Y} = 0. \quad (16c)$$

Equations (16) can be solved for a general odd integer $n \geq 3$:

$$\left. \begin{aligned} X &= \frac{1}{2} - \frac{3}{8}h^2 - \frac{1}{2}d_5Z^2 - d_7Z^3 - \frac{3}{2}d_9Z^4 - 2d_{11}Z^5 - \dots - \frac{n-3}{4}d_nZ^{\frac{n-1}{2}} \\ Y &= Z \\ d_3 &= \frac{-4+h^2}{8Z} \\ &- \left(\frac{3}{2}d_5Z + 2d_7Z^2 + \frac{5}{2}d_9Z^3 + 3d_{11}Z^4 + \dots + \left(1 + \frac{n-3}{4}\right) d_nZ^{\frac{n-3}{2}} \right) \end{aligned} \right\}, \tag{17}$$

where Z is a solution of the polynomial equation $g_n(Z) = 0$

$$g_n(Z) = 2(n-1)h^2d_nZ^{\frac{n+1}{2}} + \dots + 16h^2d_{11}Z^6 + 12h^2d_9Z^5 + 8h^2d_7Z^4 + 4h^2d_5Z^3 + (h^4 - 4h^2)Z + 8f^2 = 0. \tag{18}$$

4.2. Bifurcation set

It follows from the general theory of implicit functions that in a singular point there are multiple solutions of Eq. (8) [23, 30]. We shall use this property to compute parameters values for which the amplitude profile defined by Eq. (8) has singular points. We shall refer to such a set in the parameter space as the bifurcation set, see Ref. [27], where this term was used in the context of multiple solutions of the amplitude equation for the Duffing equation in the non-singular case.

To define a singular point, we can use Eqs. (16a) and (16b) which excludes existence of the single-valued function $X = f(Y)$ and an alternative to condition (16c) which excludes existence of the single-valued function $Y = g(X)$.

We thus solve Eqs. (16a), (16b)

$$L_n(X, Y) = 0, \tag{19a}$$

$$\frac{\partial L_n(X, Y)}{\partial X} = 0, \tag{19b}$$

obtaining

$$X = 1 - \frac{1}{2}h^2 + d_3Z + d_5Z^2 + d_7Z^3 + d_9Z^4 + d_{11}Z^5 + \dots + d_nZ^{\frac{n-1}{2}}, \tag{20a}$$

$$Y = Z, \tag{20b}$$

where Z is a solution of the polynomial equation $f_n(Z) = 0$

$$f_n(Z) = h^2d_nZ^{\frac{n+1}{2}} + \dots + h^2d_{11}Z^6 + h^2d_9Z^5 + h^2d_7Z^4 + h^2d_5Z^3 + h^2d_3Z^2 + (4h^2 - h^4)Z - f^2 = 0. \tag{20c}$$

Note that roots of the polynomial f_n are values of the amplitude function $Y = g(X)$ in critical points (*i.e.* at maxima, minima or inflexion points). Indeed, suppose that $Y = g(X)$ is a solution of Eq. (19a) and $\frac{\partial L_n(X,Y)}{\partial Y} \neq 0$. Then we have $\frac{dY}{dX} = g'(X) = -\frac{\partial L_n/\partial X}{\partial L_n/\partial Y}$ and it follows from Eq. (19b) that $g'(X) = 0$. We show that critical points shape bifurcation diagrams.

We now demand that there are multiple solutions of Eq. (20c) — these conditions, an alternative to Eq. (16c), guarantee the singularity of solutions of Eq. (16a). The necessary and sufficient condition for a polynomial to have multiple roots is that its discriminant Δ vanishes [31], see also lecture notes [32]. Discriminant Δ can be computed as a resultant of a polynomial $f(X)$ and its derivative f' with a suitable normalizing factor.

Polynomials f and g have a common root if and only if their resultant is zero. More exactly, resultant $R(f, g)$ of two polynomials, $f(X) = a_n X^n + \dots + a_1 X + a_0$, $g(X) = b_m X^m + \dots + b_1 X + b_0$, is given by a determinant of the $(m + n) \times (m + n)$ Sylvester matrix — see, for example, Eq. (1) in [32]

$$R(f, g) = \det \begin{pmatrix} a_n & a_{n-1} & a_{n-2} & \dots & 0 & 0 & 0 \\ 0 & a_n & a_{n-1} & \dots & 0 & 0 & 0 \\ \vdots & \vdots & \vdots & & \vdots & \vdots & \vdots \\ 0 & 0 & 0 & \dots & a_1 & a_0 & 0 \\ 0 & 0 & 0 & \dots & a_2 & a_1 & a_0 \\ b_m & b_{m-1} & b_{m-2} & \dots & 0 & 0 & 0 \\ 0 & b_m & b_{m-1} & \dots & 0 & 0 & 0 \\ \vdots & \vdots & \vdots & & \vdots & \vdots & \vdots \\ 0 & 0 & 0 & \dots & b_1 & b_0 & 0 \\ 0 & 0 & 0 & \dots & b_2 & b_1 & b_0 \end{pmatrix}. \tag{21}$$

Therefore, the bifurcation set $\mathcal{M}(f, h, c_3, c_5, \dots, c_n)$ for a generalized Duffing equation (2) reads

$$R(f_n, f'_n) = 0, \tag{22}$$

where the polynomial $f_n(Z)$ is defined in Eq. (20c), and parameters d_n are given in Eq. (9).

4.3. Bifurcation sets for the cubic and cubic-quintic Duffing equations

Let us first consider the cubic-quintic Duffing equation since results for the cubic Duffing equation can be easily obtained by setting $c_5 = 0$. For the cubic-quintic Duffing equation, we get from Eq. (8)

$$\begin{aligned} L_5(X, Y) &= h^2 XY + Y (X - 1 - d_3 Y - d_5 Y^2)^2 - f^2 = 0, \\ d_3 &= \frac{3}{4} c_3, \quad d_5 = \frac{5}{8} c_5, \quad (X \equiv \Omega^2, Y \equiv A^2) \end{aligned} \tag{23}$$

and it follows from Eq. (20c) that we have to consider conditions for multiple roots for the polynomial

$$f_5(Z) = aZ^3 + bZ^2 + cZ + d = 0, \\ a = 5h^2c_5, \quad b = 6h^2c_3, \quad c = (-2h^4 + 8h^2), \quad d = -8f^2. \quad (24)$$

The condition for multiple roots is (see Eqs. (21), (22))

$$R(f_5, f'_5) = \det \begin{pmatrix} a & b & c & d & 0 \\ 0 & a & b & c & d \\ 3a & 2b & c & 0 & 0 \\ 0 & 3a & 2b & c & 0 \\ 0 & 0 & 3a & 2b & c \end{pmatrix} \\ = a(4ac^3 - b^2c^2 + 4db^3 - 18abdc + 27a^2d^2) = 0. \quad (25)$$

Since the $a \neq 0$ condition for multiple (double and triple) roots is

$$4ac^3 - b^2c^2 + 4db^3 - 18abdc + 27a^2d^2 = 0, \quad (26)$$

or, after substituting expressions (24) for a, b, c, d , we get an equation defining the bifurcation set $\mathcal{M}(f, h, c_3, c_5)$

$$10c_5h^{10} + (9c_3^2 - 120c_5)h^8 + (-72c_3^2 + 480c_5)h^6 \\ + (540c_5c_3f^2 + 144c_3^2 - 640c_5)h^4 \\ + (-2160c_5 + 432c_3^2)c_3f^2h^2 - 2700c_5^2f^4 = 0. \quad (27)$$

It is now possible to find the condition for degenerate singular points. A cubic polynomial (24) has a triple root if, apart from condition (25), also f and f'' have a common root

$$R(f_5, f''_5) = \det \begin{pmatrix} a & b & c & d \\ 6a & 2b & 0 & 0 \\ 0 & 6a & 2b & 0 \\ 0 & 0 & 6a & 2b \end{pmatrix} = -8a(2b^3 - 9abc + 27da^2) = 0. \quad (28)$$

Therefore, the condition for a triple root reads

$$4ac^3 - b^2c^2 + 4db^3 - 18abdc + 27a^2d^2 = 0, \\ 2b^3 - 9abc + 27da^2 = 0 \quad (29)$$

and, after expressions for a, b, c, d (24) are invoked, the solution, defining degenerate bifurcation set $\mathcal{M}_{\text{deg}}(f, h, c_3, c_5)$, is

$$f = \pm \frac{1}{6c_3} \sqrt{-c_3} h (h^2 - 4), \quad c_5 = \frac{6c_3^2}{5(4 - h^2)}. \quad (30)$$

We can now easily extract an expression for the bifurcation set for the cubic Duffing equation. Indeed, substituting in Eq. (27) $c_5 = 0$, we get

$$9c_3^2h^2(h^6 - 8h^4 + 16h^2 + 48c_3f^2) = 0, \tag{31}$$

and thus the bifurcation set $\mathcal{M}(f, h, c_3)$ is

$$c_3 = -\frac{(h^2 - 4)^2}{48f^2}h^2, \quad (c_3 \neq 0, h \neq 0, f \neq 0). \tag{32}$$

Moreover, it follows from (30) that there are no degenerate singular points for the cubic Duffing equation.

5. Singular points of the amplitude profile for the cubic Duffing equation and the corresponding bifurcations

Substituting in Eq. (32) $h = 1, f = 1$, we compute $c_3 = -0.1875$ (the case of the softening spring) and $X = \Omega^2 = \frac{1}{8}, Y = A^2 = \frac{8}{3}$.

The corresponding amplitude profile, as well as two non-singular curves, are shown in Fig. 1. The singular curve (red) corresponds to self-intersection. The corresponding bifurcation diagrams, computed by numerical integration of the differential equation (2), $n = 3$, are shown in Fig. 2.

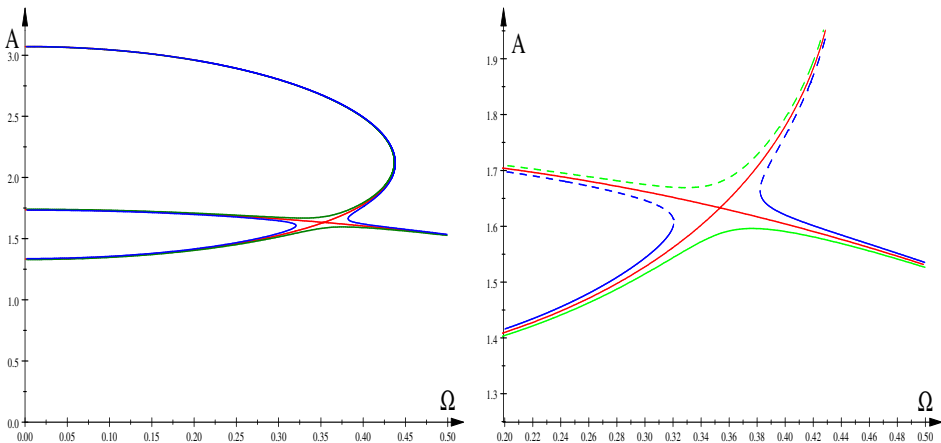


Fig. 1. (Colour on-line) Amplitude profiles, $f = 1$ (singular, red), $f = 0.999$ (green), and $f = 1.001$ (blue) — left, neighbourhood of the singular point, unstable branches marked by dashed lines — right.

It follows that there is indeed a gap on the bifurcation diagram (blue, Fig. 2), corresponding to discontinuity on the amplitude profile (blue, Fig. 1). In the case of numerical computation, the discontinuity occurred for $1.060 < f < 1.061$, is in good agreement with the predicted value $f = 1$.

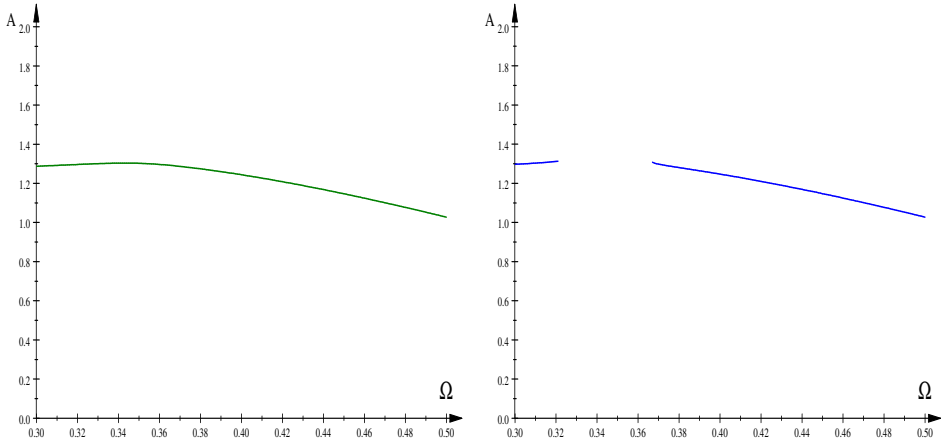


Fig. 2. (Colour on-line) Bifurcation diagrams, $f = 1.060$, left (green) and $f = 1.061$, right (blue).

6. Examples of bifurcations at singular points of the amplitude profile for the cubic-quintic Duffing equation

It follows from Eqs. (30) that the cubic-quintic equation has a degenerate singular point for $c_3 < 0$. Moreover, in the neighbourhood of this point, there are two families of non-degenerate singular points: isolated points and self-intersections.

Choosing, for example, $h = 0.2$, $c_3 = -0.2$, we compute from (30) other parameters of the degenerate singular point as $c_5 = 1.212\,121 \times 10^{-2}$, $f = 0.295\,161$ and $\Omega = 0.565\,685$, $A = 2.569\,047$.

Now, for $h = 0.2$, $c_3 = -0.2$ and $c_5 = 1.15 \times 10^{-2}$, we compute from Eqs. (16) for $n = 5$: $f = 0.282\,240$ — an isolated singular point with $\Omega = 0.472\,685$, $A = 2.920\,851$ and $f = 0.290\,089$ — a self-intersection with $\Omega = 0.617\,184$, $A = 2.319\,843$. The corresponding amplitude profiles for the degenerate and the isolated point are shown in Fig. 3. Green, blue and magenta colours have been used to show correspondence with bifurcation diagrams computed numerically near the isolated point, see Fig. 4. In the case of numerical integration of the Duffing equation (2), see Appendix D for computational details, an isolated point appears for $0.2990 < f < 0.2991$ in good agreement with the predicted value $f = 0.282\,240$.

There are three characteristic points in Fig. 3 — solutions of Eq. (24). There is a cusp of the degenerate amplitude profile (red), singular with multiplicity 3 — a triple solution of Eq. (24). Moreover, there are two interesting points on the second amplitude curve consisting of green and blue lines and magenta dot: an isolated point — singular with multiplicity 2 (magenta

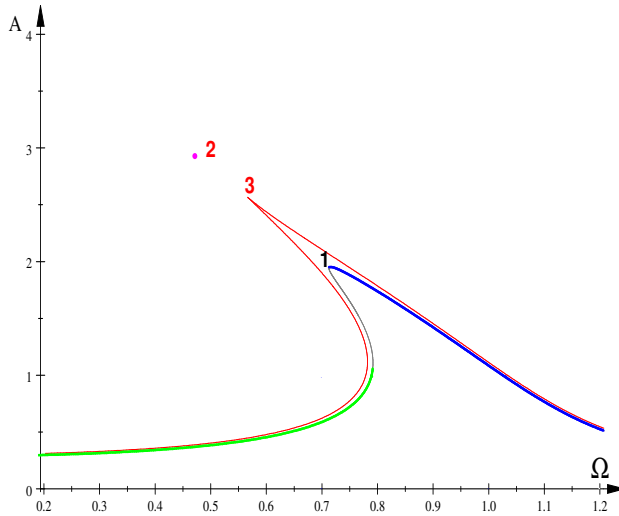


Fig. 3. (Colour on-line) Amplitude profiles: degenerate, $c_5 = 1.212\,121 \times 10^{-2}$, $f = 0.295\,161$ (red), isolated point, $c_5 = 1.15 \times 10^{-2}$, $f = 0.282\,240$ (green, blue, magenta).

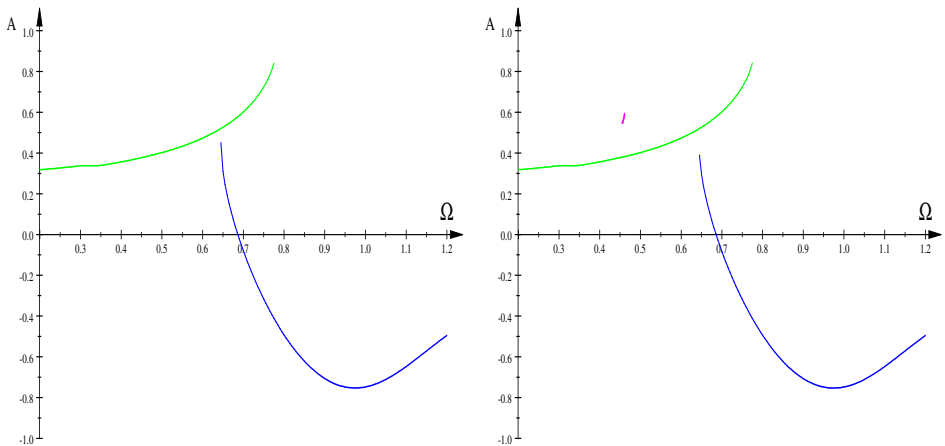


Fig. 4. (Colour on-line) Bifurcation diagrams, $f = 0.2990$ left — before the isolated point is formed, $f = 0.2991$ right — just after formation of a new branch of solution (magenta). Colours (green, blue, magenta) correspond to colours in Fig. 3.

dot) and a local maximum with multiplicity 1 — non-singular, and the corresponding bifurcation diagrams in Fig. 4 document indeed bifurcation due to metamorphosis of the amplitude profiles. The amplitude profile for the

self-intersection is shown in Fig. 5 and two amplitude profiles near the intersection are also shown in Fig. 6. The corresponding bifurcation diagrams in Fig. 7 document indeed bifurcation due to metamorphosis of the amplitude profiles.

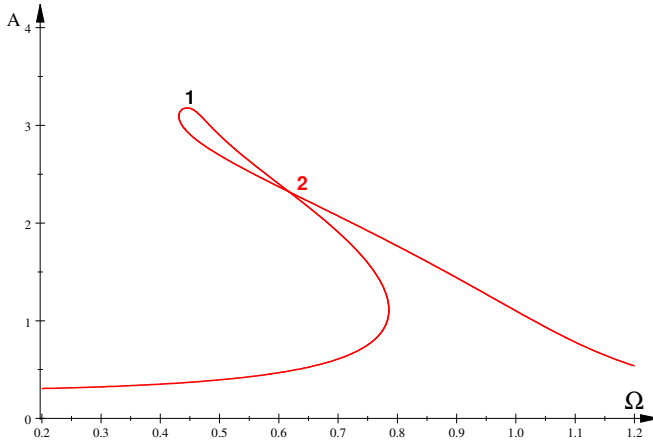


Fig. 5. Amplitude profile, $h = 0.2$, $c_3 = -0.2$, $c_5 = 1.15 \times 10^{-2}$, $f = 290\,089$.

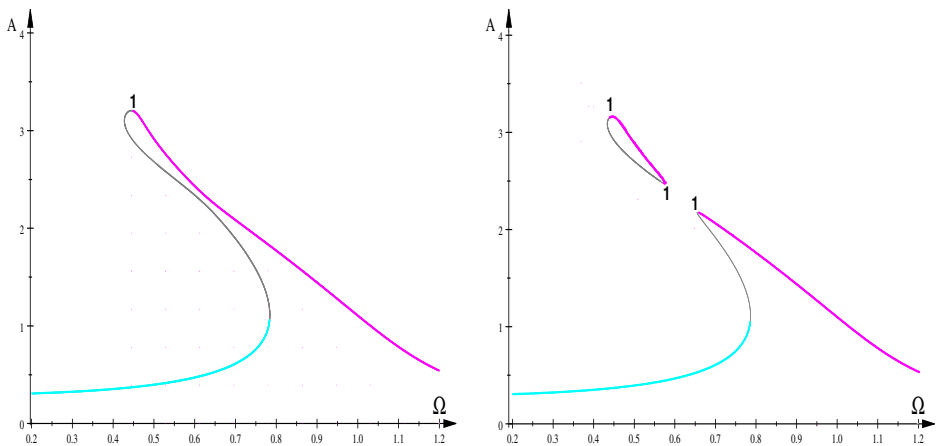


Fig. 6. Amplitude profiles, $f = 0.292$ (left, before the self-intersection), $f = 0.289$ (right, after the self intersection).

The bifurcation, discontinuity of the magenta line in the right panel of Fig. 7, appears in numerical integration of the Duffing equation for $0.3025 < f < 0.3026$ in good agreement with the predicted value $f = 0.290\,089$.

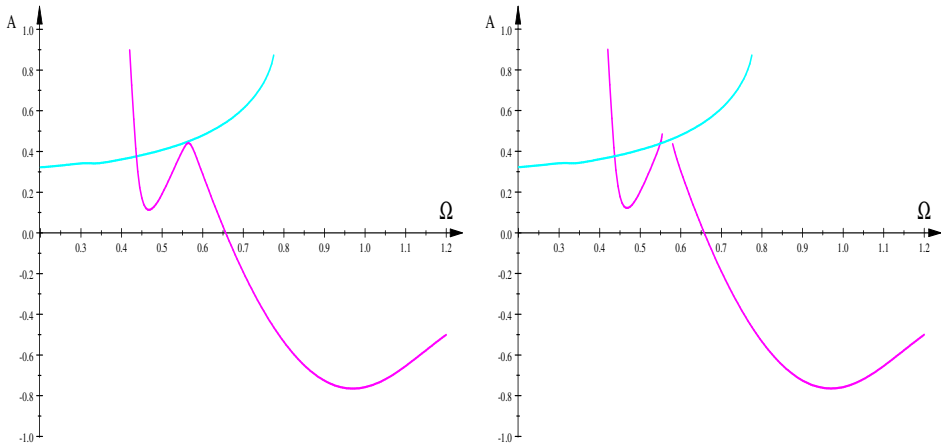


Fig. 7. Bifurcation diagrams, $f = 0.3026$ (left), $f = 0.3025$ (right).

7. Metamorphoses and bifurcations

7.1. Non-singular metamorphoses

It should be stressed that metamorphoses, *i.e.* changes of differential properties of asymptotic solutions, equivalent to bifurcations, occur also at non-singular, yet critical, points of the amplitude-response equation. To show this let us consider the jump phenomenon for the Duffing equation [2, 27], see Fig. 8. In two points marked with grey/red dots, (1.349, 0.894), (1.615, 2.058), which are solutions of Eqs. (37), metamorphoses occur — a number of branches of the asymptotic solution is changed [27]. Real so-

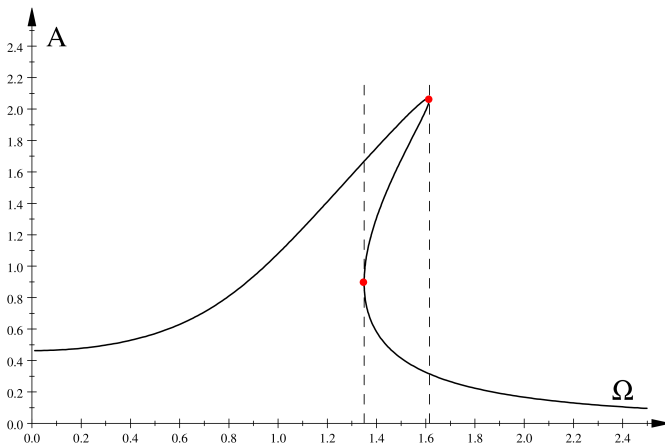


Fig. 8. Jump phenomenon for the Duffing equation, $h = 0.15$, $c_3 = 0.5$, $f = 0.5$.

lutions appear for $h < 0.304$, $c_3 = 0.5$, $f = 0.5$, see [27] for the analytical condition. It was determined by Kalmár-Nagy and Balachandran that this metamorphosis follows from a differential condition [2]

$$\frac{d\Omega}{dA} = 0, \tag{33}$$

where the amplitude-response curve for the cubic Duffing equation is $F(\Omega, A) = L_3(\Omega^2, A^2) = h^2 A^2 \Omega^2 + A^2(\Omega^2 - 1 - \frac{3}{4}c_3 A^2)^2 - f^2 = 0$ and is equivalent to the saddle-node bifurcation since one eigenvalue of the Jacobian matrix is zero, while another is negative. These metamorphoses can be also referred to as vertical tangencies of the response curve [2, 29].

Condition (33) can be formulated within the framework of an implicit function theorem. Consider the implicit amplitude-response curve

$$F(\Omega, A) = 0. \tag{34}$$

Let $\Omega = f(A)$. Then

$$\frac{\partial F}{\partial \Omega} \frac{d\Omega}{dA} + \frac{\partial F}{\partial A} \frac{dA}{dA} = 0, \tag{35}$$

and

$$\frac{d\Omega}{dA} = f'(A) = -\frac{\frac{\partial F}{\partial A}}{\frac{\partial F}{\partial \Omega}}, \quad \left(\frac{\partial F}{\partial \Omega} \neq 0 \right), \tag{36}$$

see Section 11.5 in [33].

Therefore, critical points of the function $\Omega = f(A)$, *i.e.* vertical tangencies, which follow from the Kalmár-Nagy and Balachandran condition $\frac{d\Omega}{dA} = f'(A) = 0$, fulfill an equivalent set of equations

$$F(\Omega, A) = 0, \tag{37a}$$

$$\frac{\partial F(\Omega, A)}{\partial A} = 0. \tag{37b}$$

7.2. Singular metamorphoses

Singular points of the amplitude-response curves fulfill Eqs. (13).

The first and third of these equations are conditions for vertical tangencies (37), associated with saddle-node bifurcations [2]. Therefore, because of the additional condition (13b), singular points of the amplitude-response curves lead to more complicated metamorphoses of these curves, discussed in Sections 5, 6.

On the other hand, also singular metamorphoses, due to Eq. (13c), are associated with saddle-node bifurcations. A connection between metamorphoses and bifurcations is revealed by the computation of determinant of

the Jacobian matrix \mathbb{J} . It follows from Eqs. (15), (7) that

$$\det(\mathbb{J}) = \frac{1}{4X} \frac{\partial L}{\partial Y}, \quad (38)$$

where, for simplicity, the determinant is written in variables $X = \Omega^2, Y = A^2$.

It now follows that condition $\frac{\partial L(X, Y)}{\partial Y} = 0$ (or $\frac{\partial L(\Omega^2, A^2)}{\partial A} = 0$), defining a vertical tangency, is equivalent to vanishing of the determinant $\det(\mathbb{J})$, and this means that at least one eigenvalue of the Jacobian matrix is zero, indicating a bifurcation.

We have computed another eigenvalue of the Jacobian matrix and in all cases considered it was equal to $-h$. Therefore, all the bifurcations described in Sections 5, 6 are saddle-node bifurcations of co-dimension one.

8. Summary and discussion

In this work, we have studied changes of differential properties — metamorphoses — of amplitude-response curves for the generalized Duffing equation with polynomial non-linearities (1). We have demonstrated that metamorphoses are due to formation of singular points on amplitude profiles (the case of singular metamorphoses) and due to formation of critical points on these curves (the case of non-singular metamorphoses). The non-singular case, first described in [2] as due to formation of vertical tangent points, leads to important jump phenomena [2, 27]. We discuss singular and non-singular metamorphoses and associated bifurcations in Section 7.

More precisely, we have derived formulae for singular points and bifurcation sets of the amplitude-response equation for the generalized Duffing equation (1), $n = 3, 5, 7, \dots$. We have described singular metamorphoses for the cubic Duffing equation ($n = 3$) and the cubic-quintic Duffing equation ($n = 5$).

It is interesting that there is a singular point in the case of the standard Duffing equation, see the corresponding metamorphoses of the amplitude profile and change of dynamics, *cf.* Figs. 1, 2. However, the set of parameters for which such points exist is rather small and can be easily overlooked.

In the cubic-quintic equation, $n = 5$, there are degenerate points for $c_3 < 0$ and two infinite sets of self-intersections and isolated points in the neighbourhoods of these points, see Figs. 3, 5, 6. Bifurcations diagrams show indeed changes of dynamics — the birth of new branches of solutions, Fig. 4, and the rupture of existing branches, Fig. 7.

Summing up, knowledge of metamorphoses, non-singular, as well as singular, permits prediction of changes of dynamics such as jump phenomena (due to vertical tangent points), the birth of new branches of solutions (due

to isolated points), and the rupture of existing branches of solutions leading to gaps in bifurcation diagrams (due to self-intersections). Knowledge of degenerate singular points pinpoints regions in the parameter space with families of isolated points and self-intersections where very complicated dynamical phenomena can occur.

There is an alternative approach to singular points of amplitude profiles when the implicit function can be disentangled, see Appendices A and B.

In Appendix A, we show that the implicit equation $F(A, \Omega) = 0$ can be solved for the cubic-quintic Duffing equation resulting in an explicit expression for two branches in the form of $\Omega_{\pm} = f_{\pm}(A)$ (actually Eq. (8) can be solved for Ω for any n). The condition of intersection of these branches, $f_+(A) = f_-(A)$ leads to dynamically interesting points, non-singular as well as singular. It is important that this condition, Eq. (A.2), is equivalent to the Eq. (24), derived within a more general approach. Accordingly, all these points are single or multiple solutions of Eq. (24). Within this approach, we describe metamorphoses of the amplitude profiles in a more detailed way.

We compare in Appendix B the computed amplitude profiles for the cubic-quintic Duffing equation with analogous solutions obtained by Karahan and Pakdemirli [5] within the Multiple Scales Lindstedt Poincaré (MSLP) approach, obtaining a qualitative agreement.

Finally, in Appendix C, we briefly describe how our theory can be applied to the effective equation describing plasma dynamics derived in [14].

Appendix A

*Cubic-quintic Duffing equation:
alternative approach to singular points of amplitude profiles*

Solving Eq. (23) for Ω we get two positive solutions

$$\Omega_{\pm} = \frac{1}{4} \sqrt{\frac{2}{A}} \sqrt{f(A) \pm 2\sqrt{g(A)}}, \tag{A.1a}$$

$$f(A) = 5c_5 A^5 + 6c_3 A^3 + 4A(2 - h^2), \tag{A.1b}$$

$$g(A) = -10c_5 A^6 h^2 - 12c_3 A^4 h^2 + 4A^2 h^2 (h^2 - 4) + 16f^2. \tag{A.1c}$$

Branches (A.1a) intersect for

$$g(A) = -10c_5 A^6 h^2 - 12c_3 A^4 h^2 + 4A^2 h^2 (h^2 - 4) + 16f^2 = 0. \tag{A.2}$$

It follows that $g(A) = -2f_5(A^2)$, cf. Eq. (24), and thus conditions $g(A) = 0$ and $f_5(A^2) = 0$ are equivalent.

In Figs. 9, 10, transitions from non-singular amplitude profile to self-intersection, to non-singular profile, and to an isolated point are shown for $h = 0.2$, $c_3 = -0.2$, $c_5 = 0.0115$, and values of f shown in the figures.

Branches Ω_+ and Ω_- are coloured black/blue and grey/green, respectively, black and grey/red digits in the figures denote multiplicity of the intersections of the branches (*i.e.* multiplicity of solutions of Eq. (A.2)) and correspond to non-singular and singular cases, respectively.

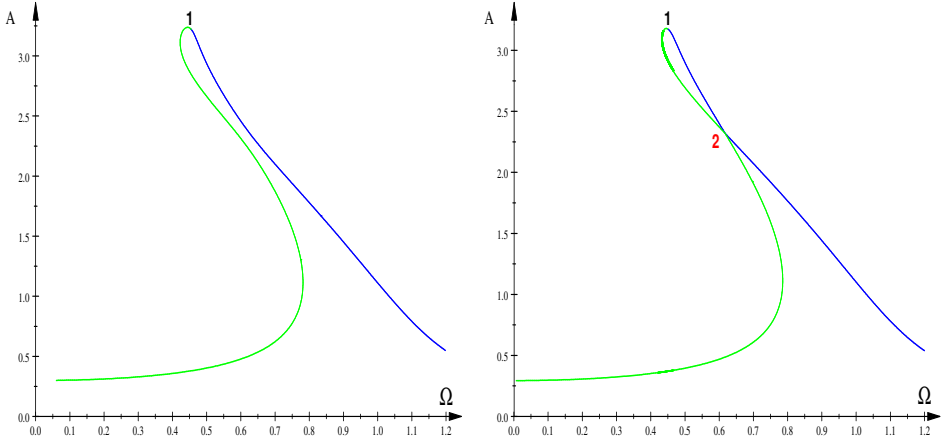


Fig. 9. (Colour on-line) Amplitude profiles: $f = 0.295$ (left), $f = 0.290\ 089$ (right).

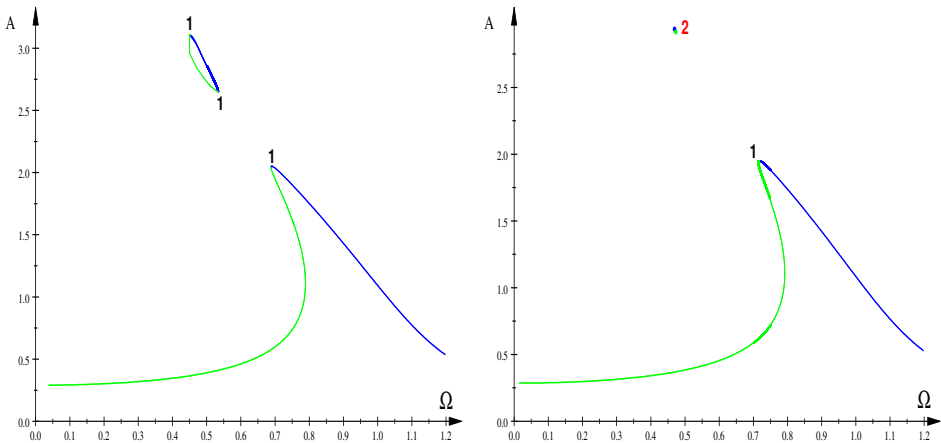


Fig. 10. (Colour on-line) Amplitude profiles: $f = 0.286$ (left), $f = 0.282\ 25$ (right).

Note that this approach works for the generalized Duffing equation (2) for any n since the amplitude equation (8) can be solved for Ω for an arbitrary n .

Appendix B

Comparison with asymptotic solution from Ref. [5]

The cubic-quintic Duffing equation was also solved by application of Multiple Scales Lindstedt Poincaré (MSLP) method by Karahan and Pakdemirli, see Eqs. (89), (90) in [5]. The authors computed the explicit solution as a function $\Omega = f(A)$ consisting of two branches

$$\frac{\Omega_{\pm}}{\omega} = 1 + \varepsilon^2 \left(\frac{3\alpha^3}{256\omega^4} A^4 + \frac{10\beta}{32\omega^2} A^4 \pm \frac{1}{2} \sqrt{\frac{F^2}{A^2\omega^4} - \left(\frac{\mu}{\omega}\right)^2} \right), \tag{B.1a}$$

$$\omega = \sqrt{1 + \varepsilon \frac{3}{4} \alpha A^2}. \tag{B.1b}$$

Parameters used in [5] and our parameters are related

$$h = \varepsilon^2 \mu, \quad c_3 = \varepsilon \alpha, \quad c_5 = \varepsilon^2 \beta, \quad f = \varepsilon^2 F. \tag{B.2}$$

The condition for intersection of these branches is:

$$\frac{F^2}{A^2\omega^4} - \left(\frac{\mu}{\omega}\right)^2 = 0. \tag{B.3}$$

In Figs. 11 and 12, $\varepsilon = 1$, $\mu = h = 0.2$, $\alpha = c_3 = -0.2$, $\beta = c_5 = 0.0115$. Grey/red digits indicate multiplicity of intersections of the branches (multiplicity of solutions of Eq. (B.3), branches ω_+ and ω_- are coloured black/blue and grey/green, respectively).

Intersection of multiplicity 2 appears for $F = f = 0.258199$ what can be compared with the value obtained by numerical integration of the cubic-quintic Duffing equation $0.3025 < f < 0.3026$ (we have obtained from the KBM implicit function (23) value $f = 290089$).

Alternatively, we can compute singular points writing Eq. (B.1a) in the form of $f(\Omega, A) = \pm \sqrt{g(\Omega, A)}$ to obtain the implicit equation of the form of $K(\Omega, A) = f^2(\Omega, A) - g(\Omega, A) = 0$ and applying standard equations

$$K(\Omega, A) = 0, \tag{B.4a}$$

$$\frac{\partial K(\Omega, A)}{\partial \Omega} = 0, \tag{B.4b}$$

$$\frac{\partial K(\Omega, A)}{\partial A} = 0. \tag{B.4c}$$

We can demonstrate within this approach that functions (B.1) have neither degenerate nor isolated points as singular solutions. It seems, however, that such points will be present if the MSLP solution contains higher-order terms.

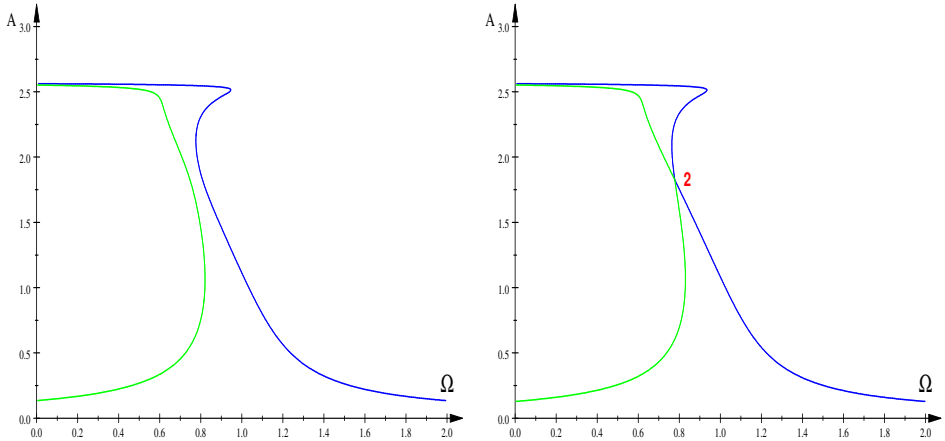


Fig. 11. (Colour on-line) Amplitude profiles: $F = f = 0.27$ (left), $F = f = 0.258199$ (right).

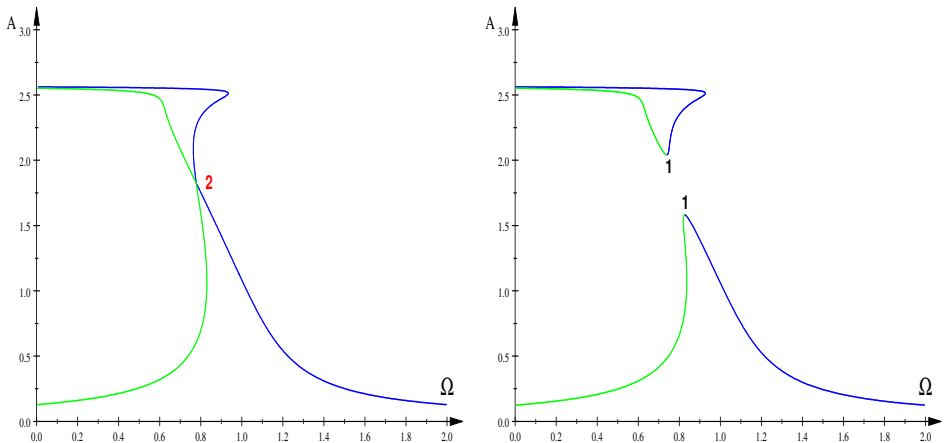


Fig. 12. (Colour on-line) Amplitude profiles: $F = f = 0.258199$ (left), $F = f = 0.25$ (right).

Appendix C

Application to plasma equations derived in Ref. [13]

In [13], the authors analyse Eq. (1) governing plasma dynamics

$$\ddot{x} + \omega_0^2 x + \beta x^2 + \alpha x^3 = E \cos(\Omega t), \quad (\text{C.1})$$

and a corresponding amplitude–frequency response equation

$$L(\Omega, A) = \frac{9}{4}\alpha^2 A^5 + \left(\frac{9}{2}\alpha\omega_0^2 - 3\alpha\Omega^2 - 2\beta\right) A^3 - 3\alpha EA^2 + 2\omega_0^2(\omega_0^2 - \Omega^2) A - 2\omega_0^2 E, \tag{C.2}$$

and find jump phenomena, see their Figs. 1, 2.

A vertical tangent bifurcation, corresponding to jump phenomenon, fulfills equation (see Subsection 7.1)

$$L(\Omega, A) = 0, \tag{C.3a}$$

$$\frac{\partial L(\Omega, A)}{\partial A} = 0. \tag{C.3b}$$

Solving equations (C.3) for A, Ω , we get the algebraic equation

$$f(A) = 27\alpha^3 A^7 + 36\alpha^2\omega_0^2 A^5 + 18\alpha^2 EA^4 + (-16\omega_0^2\beta + 12\alpha\omega_0^4) A^3 + 24\alpha\omega_0^2 EA^2 + 8\omega_0^4 E. \tag{C.4}$$

To find parameter values for which such bifurcations occur (the bifurcation set), we can solve the equation

$$R(f, f') = 0, \tag{C.5}$$

where $R(f, f')$ is the resultant (21), since then the number of branches of solutions changes and the polynomial $f(Z)$ has multiple solutions, see Fig. 8. Equation (C.5) for the polynomial (C.4) yields

$$\begin{aligned} & -65\,536\omega_0^8\beta^5 + 245\,760\alpha\omega_0^{10}\beta^4 + (710\,912\alpha^3\omega_0^6E^2 - 368\,640\alpha^2\omega_0^{12})\beta^3 \\ & + (5298\,048\alpha^4\omega_0^8E^2 - 6561\alpha^5\omega_0^2E^4 + 276\,480\alpha^3\omega_0^{14})\beta^2 \\ & + (2733\,264\alpha^5\omega_0^{10}E^2 - 1335\,528\alpha^6\omega_0^4E^4 - 103\,680\alpha^4\omega_0^{16})\beta \\ & + 52\,488\alpha^8E^6 + 104\,976\alpha^7\omega_0^6E^4 + 69\,984\alpha^6\omega_0^{12}E^2 + 15\,552\alpha^5\omega_0^{18} = 0. \end{aligned} \tag{C.6}$$

For example, for $\omega_0 = 1, \alpha = 0.5, E = 0.1$, we compute from (C.6) the critical value of $\beta, \beta_{cr} = 0.965\,996\,8$, see Fig. 13 where emergence of jump phenomenon is shown (the grey/green curve can be compared with the bottom curve in Fig. 2 in [13]).

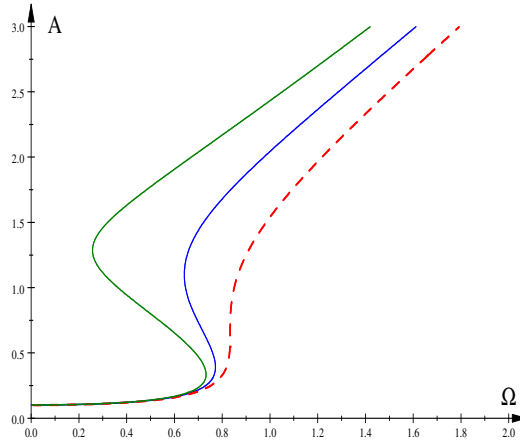


Fig. 13. (Colour on-line) Amplitude profiles: $\beta = \beta_{cr}$ (dashed/red), $\beta = 1.5$ (black/blue), $\beta = 2$ (grey/green).

Appendix D

Computational details

Nonlinear polynomial equations were solved numerically using the computational engine Maple 4.0 from the Scientific WorkPlace 4.0. Figures were plotted with the computational engine MuPAD 4.0 from Scientific WorkPlace 5.5. Curves shown in bifurcation diagrams in Figs. 2, 4, 7 were computed by integrating numerically Eq. (2), $n = 3, 5$, running DYNAMICS, program written by H.E. Nusse and J.A. Yorke [34], and our own programs written in Pascal.

REFERENCES

- [1] I. Kovacic, M.J. Brennan (Eds.) «The Duffing Equation: Nonlinear Oscillators and Their Behavior», *John Wiley & Sons, 2011*.
- [2] T. Kalmár-Nagy, B. Balachandran, «Forced harmonic vibration of a Duffing oscillator with linear viscous damping», in: «The Duffing Equation: Nonlinear Oscillators and Their Behavior», *John Wiley & Sons, 2011*, pp. 139–174.
- [3] Asok Kumar Mallik, «Forced harmonic vibration of a Duffing oscillator with different damping mechanisms», in: «The Duffing Equation: Nonlinear Oscillators and Their Behavior», *John Wiley & Sons, 2011*, pp. 175–217.

- [4] D. Younesian, H. Askari, Z. Saadatnia, M. Kalami Yazdi, «Frequency analysis of strongly nonlinear generalized Duffing oscillators using He's frequency-amplitude formulation and He's energy balance method», *Comput. Math. Appl.* **59**, 3222 (2010).
- [5] M.M. Fatih Karahan, M. Pakdemirli, «Free and forced vibrations of the strongly nonlinear cubic-quintic Duffing oscillators», *Zeit. Natur. A* **72**, 59 (2017).
- [6] I. Khatami, Zahedi Ehsan, Zahedi Mohsen, «Efficient Solution of Nonlinear Duffing Oscillator», *J. Appl. Comput. Mech.* **6**, 219 (2020).
- [7] D.V. Hieu, N.Q. Hai, «Analyzing of nonlinear generalized Duffing oscillators using the equivalent linearization method with a weighted averaging», *Asian Res. J. Math.* **9**, 1 (2018).
- [8] A. Azimi, M. Azimi, «Computing Simulation of the Generalized Duffing Oscillator Based on EBM and MHPM», *Mech. Mech. Eng.* **20**, 595 (2016).
- [9] D. Zulli, A. Luongo, «Control of primary and subharmonic resonances of a Duffing oscillator via non-linear energy sink», *Int. J. Nonlinear Mech.* **80**, 170 (2016).
- [10] M. Bikdash, B. Balachandran, A.H. Navfeh, «Melnikov analysis for a ship with a general roll-damping model», *Nonlinear Dyn.* **6**, 101 (1994).
- [11] M. Pandey, R.H. Rand, A.T. Zehnder, «Frequency locking in a forced Mathieu–van der Pol–Duffing system», *Nonlinear Dyn.* **54**, 3 (2008).
- [12] F. Tajaddodianfar, M.R.H. Yazdi, H.N. Pishkenari, «Nonlinear dynamics of MEMS/NEMS resonators: analytical solution by the homotopy analysis method», *Microsyst. Technol.* **23**, 1913 (2017).
- [13] H.G. Enjieu Kadji, J.B. Chabi Orou, P. Woafu, «Regular and chaotic behaviors of plasma oscillations modeled by a modified Duffing equation», *Phys. Scr.* **77**, 025503 (2008).
- [14] H.G. Enjieu Kadji, B.R. Nana Nbandjo, J.B. Chabi Orou, P.K. Talla, «Nonlinear dynamics of plasma oscillations modeled by an anharmonic oscillator», *Phys. Plasmas* **15**, 032308 (2008).
- [15] H.G. Enjieu Kadji, B.R. Nana Nbandjo, «Passive aerodynamics control of plasma instabilities», *Commun. Nonlinear Sci.* **17**, 1779 (2012).
- [16] B. Baumann *et al.*, «Nonlinear behavior in high-intensity discharge lamps», *J. Phys. D: Appl. Phys.* **49**, 255201 (2016).
- [17] A.H. Salas, S.A. El-Tantawy, «On the approximate solutions to a damped harmonic oscillator with higher-order nonlinearities and its application to plasma physics: semi-analytical solution and moving boundary method», *Eur. Phys. J. Plus* **135**, 833 (2020).
- [18] V.P. Chua, M.A. Porter., «Spatial resonance overlap in Bose–Einstein condensates in superlattice potentials», *Int. J. Bifur. Chaos* **16**, 945 (2006).

- [19] M. Van Noort, M.A. Porter, Y. Yi, S.N. Chow, «Quasiperiodic Dynamics in Bose–Einstein Condensates in Periodic Lattices and Superlattices», *J. Nonlinear Sci.* **17**, 59 (2007).
- [20] C. Ainamon, C.H. Miwadinou, A.V. Monwanou, J.C. Orou, «Analysis of multiresonance and chaotic behavior of the polarization in materials modeled by a Duffing equation with multifrequency excitations», *Appl. Phys. Res.* **6**, 74 (2014).
- [21] B.M. Mihalcea, G.G. Vişan, «Nonlinear ion trap stability analysis», *Phys. Scr.* **T140**, 014057 (2010).
- [22] A.H. Nayfeh, «Introduction to Perturbation Techniques», *John Wiley & Sons*, 2011.
- [23] J. Kyzioł, A. Okniński, «Effective equation for two coupled oscillators: Towards a global view of metamorphoses of the amplitude profiles», *Int. J. Nonlinear Mech.* **123**, 103495 (2020).
- [24] J. Kyzioł, A. Okniński, «Coupled nonlinear oscillators: metamorphoses of amplitude profiles. The case of the approximate effective equation», *Acta Phys. Pol. B* **42**, 2063 (2011).
- [25] M. Spivak, «Calculus on Manifolds», *W.A. Benjamin, Inc.*, Menlo Park, California 1965.
- [26] C.T.C. Wall, «Singular Points of Plane Curves», *Cambridge University Press*, New York 2004.
- [27] P.J. Holmes, D.A. Rand, «The bifurcations of duffing’s equation: An application of catastrophe theory», *J. Sound Vib.* **44**, 237 (1976).
- [28] J. Awrejcewicz, «J. Modified Poincaré method and implicit function theory», in: J. Awrejcewicz (Ed.) «Nonlinear Dynamics: New Theoretical and Applied Results», *Akademie Verlag*, Berlin 1995.
- [29] A.H. Nayfeh, B. Balachandran, «Applied Nonlinear Dynamics: Analytical, Computational, and Experimental Methods», *John Wiley & Sons*, 2008.
- [30] J. Kyzioł, A. Okniński, «Van der Pol–Duffing oscillator: Global view of metamorphoses of the amplitude profiles», *Int. J. Nonlinear Mech.* **116**, 102 (2019).
- [31] I.M. Gelfand, M.M. Kapranov, A.V. Zelevinsky, «Discriminants, Resultants, and Multidimensional Determinants», *Springer Science & Business Media*, 2008.
- [32] S. Janson, «Resultant and discriminant of polynomials», lecture notes, <http://www2.math.uu.se/~char126/relaxsvante/papers/sjN5.pdf>, 2010.
- [33] J. Stewart, «Calculus: Concepts and Contexts», *Brooks/Cole*, Cengage Learning, 2009.
- [34] H.E. Nusse, J.A. Yorke, «Dynamics: Numerical Explorations», *Springer Verlag*, New York 1997.